Chemical Science

ROYAL SOCIETY OF CHEMISTRY

EDGE ARTICLE

View Article Online
View Journal | View Issue

Cite this: *Chem. Sci.*, 2021, **12**, 13045

All publication charges for this article have been paid for by the Royal Society of Chemistry

The mechanism of oxidative addition of Pd(0) to Si–H bonds: electronic effects, reaction mechanism, and hydrosilylation†

Michael R. Hurst, Lev N. Zakharov and Amanda K. Cook *

The oxidative addition of Pd to Si–H bonds is a crucial step in a variety of catalytic applications, and many aspects of this reaction are poorly understood. One important yet underexplored aspect is the electronic effect of silane substituents on reactivity. Herein we describe a systematic investigation of the formation of silyl palladium hydride complexes as a function of silane identity, focusing on electronic influence of the silanes. Using $[(\mu\text{-dcpe})Pd]_2$ (dcpe = dicyclohexyl(phosphino)ethane) and tertiary silanes, data show that equilibrium strongly favours products formed from electron-deficient silanes, and is fully dynamic with respect to both temperature and product distribution. A notable kinetic isotope effect (KIE) of 1.21 is observed with $H/DSiPhMe_2$ at 233 K, and the reaction is shown to be 0.5^{th} order in $[(\mu\text{-dcpe})Pd]_2$ and 1^{st} order in silane. Formed complexes exhibit temperature-dependent intramolecular H/Si ligand exchange on the NMR timescale, allowing determination of the energetic barrier to reversible oxidative addition. Taken together, these results give unique insight into the individual steps of oxidative addition and suggest the initial formation of a σ-complex intermediate to be rate-limiting. The insight gained from these mechanistic studies was applied to hydrosilylation of alkynes, which shows parallel trends in the effect of the silanes' substituents. Importantly, this work highlights the relevance of in-depth mechanistic studies of fundamental steps to catalysis.

Received 12th August 2021
Accepted 3rd September 2021

DOI: 10.1039/d1sc04419b

rsc.li/chemical-science

Introduction

Palladium hydrides are a unique class of organometallic compounds[1,2] which are invoked as key intermediates in a variety of catalytic reactions, including the Mizoroki–Heck reaction,[3–5] alcohol and alkene oxidation,[6–8] nucleocarbonylation reactions, hydrofunctionalization reactions,[9] (co)polymerization reactions,[10,11] and alkene and alkyne (cyclo) isomerization reactions.[12–14] However, despite the fact that these species are often proposed as intermediates, the direct observation or isolation of complexes containing a formal Pd–H bond is uncommon, and fundamental study of their behaviour has largely been precluded.[1,2,12]

Organosilicon compounds are broadly significant, since they are used as monomers to synthesize polysiloxanes (silicones),[15,16] and they have also recently gained attention for their use as biocompatible yet non-natural carbon isosteres[17] in the synthesis of bioactive molecules.[18–20] Transition metal-catalysed hydrosilylation of alkenes and alkynes is the primary method for synthesizing organosilanes,[21–25] with most development and mechanistic work focusing primarily on Pt catalysts.[22,25,26] On the other hand, Pd catalysts show complementary and modular regioselectivity[25,27,28] and are more useful in enantioselective hydrosilylation.[29–32]

A key step in the mechanism of transition metal-catalysed hydrosilylation is the oxidative addition of the metal to the Si–H bond.[21–23,25,26,33–35] While this fundamental step of organometallic chemistry, to form (silyl)M(H) complexes, has been well-studied for Pd's neighbouring elements Rh,[36–48] Pt,[49–64] and most other transition metals,[33–35] it is much less understood for Pd. The oxidative addition of Rh and Pt to Si–H is facile, and complexes have been reported with a variety of ligand scaffolds and silanes. In addition to hydrosilylation (Fig. 1b), the oxidative addition of Pd to Si–H bonds (Fig. 1a) is a vital step of carbene insertion reactions (Fig. 1c),[65–67] C–Si cross-coupling reactions (Fig. 1d),[68,69] and hydrodehalogenation reactions (Fig. 1e),[70–75] amongst others.[76–81] *A key limitation that unifies all of these reactions is the dependence on silane identity*; most reactions are heavily dependent on the number of substituents (primary *vs.* secondary silanes, *etc.*) on silicon, and most protocols do not investigate the electronic and/or steric effects of the silane substituents. Notably, the electronic effects of the silane substituents have been experimentally investigated for Rh and Pt,[37,44,46,61] but remain unexplored for Pd. Because of the importance of this step in many Pd-catalysed reactions, we

Department of Chemistry and Biochemistry, University of Oregon, Eugene, OR 97403, USA. E-mail: akcook@uoregon.edu

† Electronic supplementary information (ESI) available: Figures, schemes, tables and graphs, experimental procedures, characterization, and NMR and IR spectra. CCDC 2086211. For ESI and crystallographic data in CIF or other electronic format see DOI: 10.1039/d1sc04419b

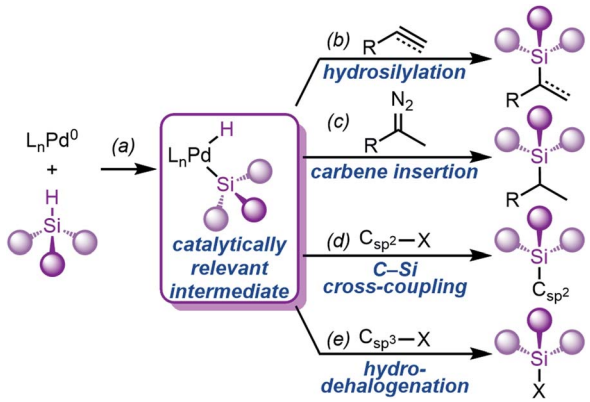

Fig. 1 (a) Oxidative addition to form silyl palladium hydride species implicated in (b) hydrosilylation (only one isomer shown for clarity), (c) carbene insertion, (d) C–Si cross-coupling, and (e) hydro-dehalogenation reactions.

sought to determine the mechanism of Si–H oxidative addition to Pd(0) with a focus on elucidating the effect of silane substituents.

Despite being implicated as catalytic intermediates for more than half of a century, it was not until the early 2000's that the Fink group reported the isolation of the first (silyl)Pd(H) complex.[82,83] Since this seminal work, Ishii[84] and Iluc[85,86] have both also published related work. Importantly, the effect of silane substituent has not been systematically explored; the silane substituents were restricted to alkyl and phenyl groups (Fig. 2a), yet trends found computationally suggest that inductive electronic effects of silane substituents dictate reactivity.[87,88] Furthermore, while some characteristics of the (silyl)Pd(H) compounds were investigated, the overall reaction mechanism remains unsupported with experimental evidence. The Si–H bond is relatively non-polar, and consequently, the mechanism of the reaction likely proceeds through a concerted pathway.[33–35] Experimental evidence to support this hypothesis is needed, including the identification of the precise rate-limiting step. Related work with Ni, Rh, and Pt complexes has shown that oxidative addition with these metals proceeds *via* a concerted oxidative addition mechanism. The formed complexes show similar characteristics; (silyl)Pt^{II}(H) complexes exhibit square planar geometry and are proposed to undergo fluxional exchange of the ligands *via* transient η^2-H–SiR_3 species.[61] This fluxional behaviour is also proposed for related Ni complexes.[89–92] A large variety of Rh complexes have been studied for oxidative addition with silanes,[33–48] and the mechanism has been elucidated in detail as well.[46]

Elucidation of the details of the reaction mechanism is also relevant in the context of the oxidative addition of C–H bonds, since Si–H bonds often react analogously; however, Si–H bonds are more basic and therefore more reactive with transition metals. Taking advantage of this reactivity difference, studying Si–H oxidative addition can offer unique insight into the oxidative addition of C–H bonds. *One important challenge in studying the mechanism of oxidative addition of non-polar bonds is decoupling the individual steps of the oxidative addition process*, which is composed of coordination and oxidative cleavage steps (Fig. 2b). Examining Si–H oxidative addition reactions offers a chance to address that challenge. Ground-breaking work by Jones[93] and Parkin[94] has investigated the reverse of oxidative addition: reductive elimination of C–H bonds using KIEs and EIEs as tools to decouple the reductive cleavage and dissociation steps.

Lastly, the known (silyl)Pd(H) compounds have yet to be shown to be relevant to catalysis. In this report, *we fill in the crucial gaps in knowledge regarding the (i) effect of silane electronics on the thermodynamics and kinetics, (ii) overall reaction mechanism, and (iii) relevance to catalysis (namely hydrosilylation) of silane oxidative addition.* Using a variety of mechanistic tools ranging from van't Hoff and Eyring analyses to competition experiments to rate and order studies, we discuss the overall reaction mechanism and the contribution of silane electronics to reactivity. These results are then shown to be relevant in the hydrosilylation of alkynes and provide mechanistic rational behind observed changes in reactivity.

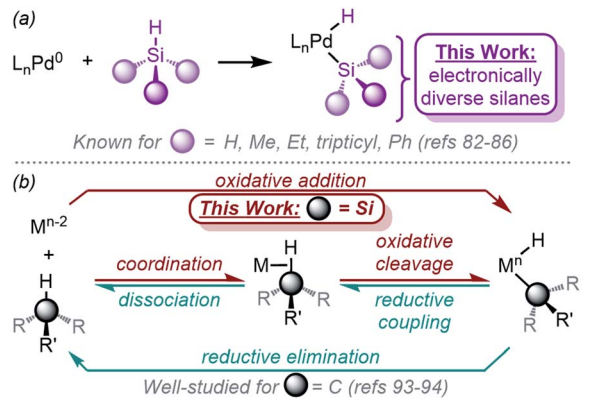

Fig. 2 (a) Previously examined silanes for oxidative addition with Pd, and (b) mechanistic relationship between oxidative addition of Si–H and reductive elimination of Si–H and C–H bonds.

Results and discussion

Initial reactivity studies of [(μ-dcpe)Pd]$_2$ (1) with silanes

We began by investigating the reactivity of a library of tertiary silanes with [(μ-dcpe)Pd]$_2$ (**1**) by ^{1}H and ^{31}P NMR (Fig. 3). These reactions proceed cleanly to afford a new product, as initially observed by NMR, and only the reactants and the product are observed. For silanes with at least one phenyl ring or alkoxide substituent (**3–6**), the reactions proceed in good to excellent conversions, but peralkyl-substituted silanes (**2**) are unreactive.

In the ^{1}H NMR spectrum, the peak corresponding to silane Si–H (4–6 ppm) is consumed during the reaction, along with concomitant appearance of a new resonance below 0 ppm (−1.23 to −2.34 ppm), which is consistent with the Pd centre interacting with the silane Si–H bond to form a (silyl)Pd(H), a Pd(η^2-H–SiR_3) complex, or some structure in between these extremes.[33–35,95,96] In addition to the ^{1}H NMR signal, a new band in the IR spectrum (1838 to 1881 cm^{-1}) is observed, consistent with known analogous Ni and Pd complexes.[91,92,97] The hydride

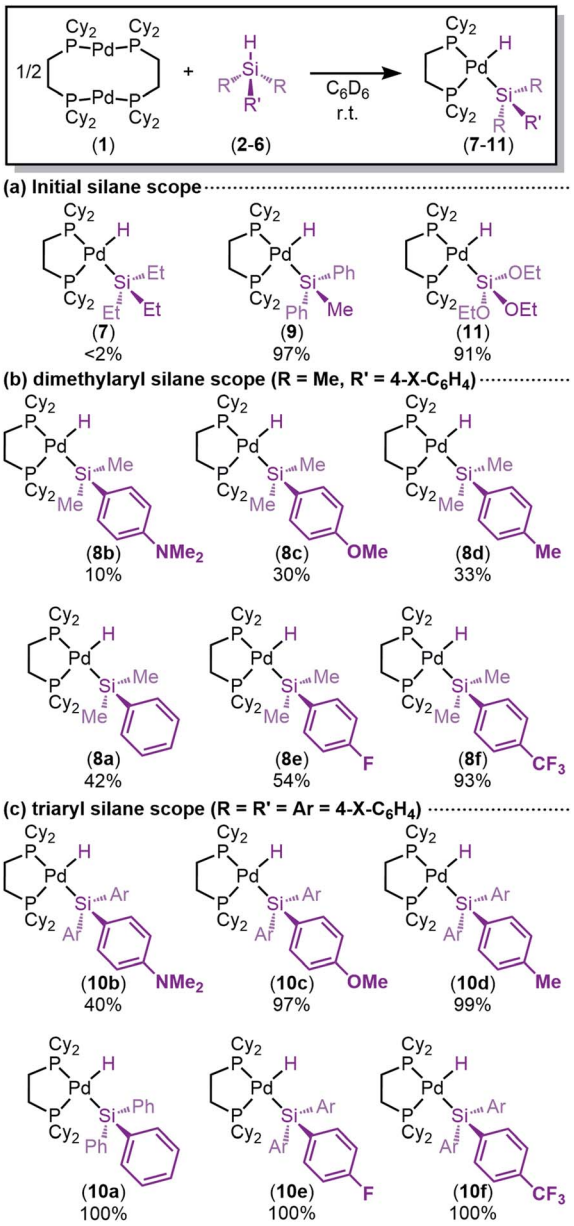

Fig. 3 Scope of silane reactivity in oxidative addition with [(μ-dcpe)Pd]$_2$ (**1**). Percent conversions were determined by NMR integrations. Reaction conditions: 1.00 equiv. of **1**, 2.05 equiv. of **2–6**, 13.33 mM in C_6D_6, and 4–6 h. (a) Initial silane scope. (b) Scope of electronically diverse dimethylaryl silanes. (c) Scope of electronically diverse triaryl silanes.

signal in the ^{1}H NMR spectrum for most products appears as a triplet at room temperature with $^2J_{H-P}$ values of 75–80 Hz, which is the average of the *cis* and *trans* coupling constants. Only one signal in the $^{31}P\{^1H\}$ NMR spectrum is observed (55–60 ppm, corresponding to a downfield shift from **1** at 23 ppm), showing that there is only one phosphorus environment. At low temperatures, the hydride signal in the ^{1}H NMR resolves into a doublet ($^2J_{H-P(trans)} = \sim 160$ Hz), the $^{31}P\{^1H\}$ spectra show two signals between 57–64 ppm, and in the ^{1}H-coupled ^{31}P spectra, the upfield signal is a doublet due to *trans* coupling to the hydride. Values for $^2J_{H-P(cis)}$ were in most cases too small to measure (<8 Hz). These NMR data are consistent with a Pd–H complex that is undergoing dynamic exchange (*vide infra*), as has been shown for related complexes.[61,82,89] The chemical shift and coupling patterns of the hydride and phosphorus signals align well with related Pd and Pt hydrides stabilized by bidentate phosphine ligands.[54,63,82,83] To distinguish where our products lie on the spectrum from σ-complex to (silyl)Pd(H), the NMR spectra of the product from reaction of **1** and **5a** ($HSiPh_3$) were analysed in more detail. The hydride peak in the ^{1}H NMR shifts from 5.71 ppm in **5a** to −1.74 ppm upon coordination/oxidative addition to Pd and changes from a singlet with ^{29}Si satellites ($J_{H-Si} = 198$ Hz) to a triplet ($^2J_{H-P} = 78$ Hz) with ^{29}Si satellites ($J_{H-Si} = 30$ Hz; see ESI, Table S1†). In related Ni,[89,91] and Pt,[61] and Rh complexes,[41,46,98,99] H–Si coupling constants were used to determine whether the complex is the result of oxidative addition to form the (silyl)M(H), or formation of the σ-complex: coupling constants smaller than 20 Hz support the formation of (silyl)M(H) and larger than ∼70 Hz support non-classical interactions.[96] The J_{H-Si} values of our complexes are in between these markers yet are closer to values known for (silyl)M(H) complexes of group 10 metals[61,82,89,91,92] than for their σ-complexes.[62,100–103] Therefore, our data support the formation of the (silyl)Pd(H) complexes, as drawn in Fig. 3.

A comparison of the data shown in Fig. 3 reveals that higher conversions are obtained with increasing number of aryl substituents and alkoxide substituents on the silane. This trend correlates well with the electronegativity of the atoms attached to Si (**11** > **10a** > **9** > **8a** > 7).[104] While this trend is revealing, we sought to decouple the kinetic effects from the thermodynamic effects and systematically investigate the electronic influence on each parameter of the reaction.

Electronic effects in oxidative addition of Pd(0) to silanes

To probe our hypothesis that the oxidative addition of silanes to Pd(0) is more facile with electron-poor silanes, a library of electronically diverse triarylsilanes were synthesized and evaluated in the reaction. The targeted silanes span a gradient of electronic character, with substituents in the *para* position ranging from electron-donating (X = NMe_2, OMe, Me) to electron-withdrawing (X = F, CF_3). Reactions of these silanes **5** with **1** cleanly yield the expected (dcpe)Pd(H)($SiAr_3$) complexes **10a–f** (Fig. 3c), all in excellent NMR conversions except for the reaction with the electron-rich 4-dimethylaminophenyl-substituted silane (**5b** → **10b**, mass balance is remaining starting material).

A translucent, off-white crystal of (dcpe)Pd(H)(Si(4-CF_3-Ph)$_3$) (**10f**) suitable for single crystal diffraction was grown from a reaction mixture of **1** and HSi(4-CF_3-Ph)$_3$ (**5f**) in benzene/hexane (Fig. 4). Product **10f** displays nearly ideal square planar geometry around the palladium atom, with the summed total of bond angles equal to 360°. To get a more precise measure of the structure's geometry, the structural parameter τ_4 was calculated from crystallographic data.[105,106] Analysis of **10f** gives $\tau_4 = 0.15$, where $\tau_4 = 0$ indicates an ideally square planar complex, and $\tau_4 = 1$ represents a tetrahedral complex. The τ_4

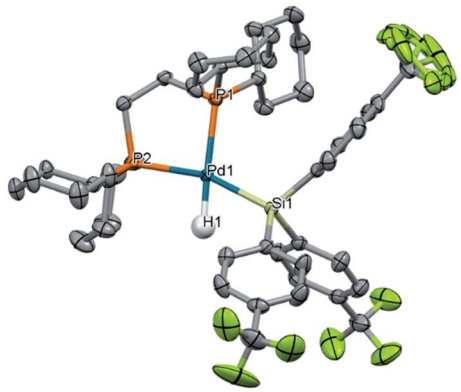

Fig. 4 Molecular structure of (dcpe)Pd(H)(Si(4-CF_3-Ph)$_3$) (**10f**). Thermal ellipsoids are drawn at 50% probability level. Hydrogen atoms except for Pd–H are omitted for clarity. Selected bond lengths (Å) and angles (deg): Pd1–H1 1.59(3), Pd1–Si1 2.3413(5), Pd1–P1 2.3422(5), Pd1–P2 2.3584(5), H1–Pd1–Si1 67(1), H1–Pd1–P2 96(1), P1–Pd1–P2 86.46(2), P1–Pd1–Si1 111.01(2). One CF_3 group is highly disordered and was refined as being located in three positions with an occupation factor of 0.33 each.

value of **10f** can be compared to similar complexes whose characterization includes the Pd–H bond length (allowing calculation of τ_4): Ishii's (dcpe)Pd(H)(SiH_2Trip) (Trip = 9-triptycyl)[84] complex gives $\tau_4 = 0.11$ and Iluc's (P–P)Pd(H)($SiHPh_2$) complex gives $\tau_4 = 0.39$ (Table S44†).[86] **10f** is therefore comparable to known square planar silyl palladium hydride complexes. Deviation from square planarity is likely due to steric repulsion between the cyclohexyl substituents of dcpe and the aryl groups of the silane.

Solid-state geometry also gives information on the strength of each ligand's *trans* influence. Silyl ligands are known for being among the strongest *trans*-influencing ligands.[107–109] Therefore, we expect that the Pd–P bond *trans* to the silyl ligand will be longer than the Pd–P bond *trans* to the H; indeed, this is the case for complex **10f**, which has Pd–P bond lengths of 2.3584(5) Å and 2.3422(5) Å, respectively.

Comparing the Pd–P bond lengths in related complexes gives insight into the *trans*-influencing ability of the 4-CF_3-phenyl substituents of the silane. The Pd–P bond length *trans* to the silyl ligand in complex **10a** (ref. 82) and Ishii's complex[84] are 2.350(2) Å and 2.3319(14) Å, respectively. With no change in ancillary ligand (dcpe) across all three cases, these results indicate that the –Si(4-CF_3–Ph)$_3$ group has a stronger *trans* influence than the –$SiPh_3$ group, which in turn is stronger than –SiH_2Trip.

Returning to our hypothesis on the effect of electronic character of the silane on oxidative addition, no useful distinctions could be made using the data in Fig. 3c, as most triaryl silanes exhibit similar reactivity. We thus turned to less reactive dimethylaryl silanes to further probe the influence of silane electronics on oxidative addition. The reaction of each dimethylaryl silane with **1** yielded the desired products (**8a–f**) (Fig. 3b), though to lower conversion than with triaryl silanes. The formed (silyl)Pd(H) complexes exhibit similar spectroscopic characteristics as described for their triaryl counterparts. The data in Fig. 3b show a clear trend with respect to the electronic nature of the silane: more electron-poor silanes give higher conversions to the silyl palladium hydrides **8**.

Reaction equilibrium

To embark upon mechanistic studies, we first sought to determine if this oxidative addition reaction is reversible or irreversible. **1** and **3a** were reacted in an NMR tube at 298 K and allowed to reach equilibrium (Fig. S10†). The reaction was then cooled to 253 K, and the conversion of **8a** was measured to be 88%. Warming the reaction to 293 K and then 333 K resulted in concomitant decreases in conversion to **8a** (44% and 17%, respectively). Subsequent cooling back to 298 K resulted in a conversion of 41%, which is consistent with the data in Fig. 3. Because the conversion is consistently ~42% at ambient temperature independent of whether the reaction had previously been heated or cooled, we deemed this reaction to be reversible.

We also tested reversibility by taking advantage of the differential reactivity of electron-rich and -poor silanes: if the reaction is indeed reversible, then we expect that a silyl palladium hydride formed from an electron-rich silane should convert to the corresponding product of oxidative addition of an electron-poor silane if one is added. This reaction is expected to occur through reductive elimination of the electron-rich silane, followed by preferential oxidative addition of the electron-poor silane. (dcpe)Pd(H)(Si(4-tolyl)$_3$) (**10d**, formed *in situ* from **1** and **5d**) was reacted with triphenyl silane (**5a**), and conversion to an equilibrium mixture of 1 : 3.3 (**10d**/**10a**) was observed (Scheme 1). An analogous experiment with *tris*(4-fluorophenyl)silane (**5e**) added to a solution of pre-formed **10a** shows an equilibrium ratio of 1 : 2.8 (**10a**/**10e**) (Table S16†). The formation of H_2 or *bis*-silyl by-products was not observed, and mass balance is consistently 100% against an internal standard. These data imply that the formation of silyl palladium hydrides is completely reversible with respect to product distribution.

To quantify the trend imparted by silane electronic character, we measured the equilibrium constants (K_{eq}) for the reactions of **1** with each silane **3a–f** and constructed a Hammett plot. This analysis gave a sensitivity constant, ρ_{eq} (eq indicates that this value is derived from equilibrium constants, as

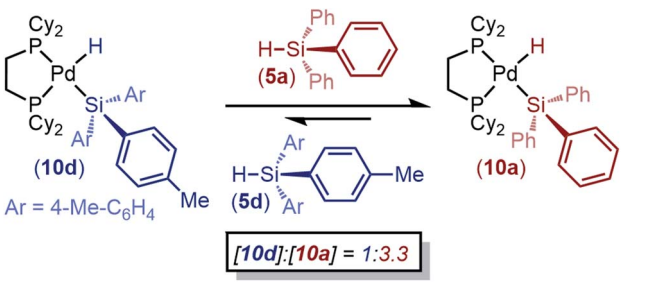

Scheme 1 Conversion of **10d** into **10a** *via* reversible oxidative addition. Experiment was performed in C_7D_8 and relative conversions were determined by $^{31}P\{^1H\}$ NMR integration; Reaction conditions: 1.00 equiv. of **1**, 2.05 equiv. each of **5a** and **5d**, 13.33 mM in C_7D_8, and 3 h.

opposed to rates of reaction) of 3.5 ± 0.5 (Fig. 5), consistent with the data in Fig. 3b showing that the reaction is more favourable with electron-poor silanes.

We hypothesized that this observed trend in K_{eq}, and thus ΔG_{OA} (OA, oxidative addition), of the reaction is dictated by the varying bond strengths of the Pd–Si bonds, where stronger Pd–Si bonds are formed with electron-poor silanes. To deconvolute the enthalpic and entropic contributions to ΔG_{OA}, the equilibrium constants as a function of temperature were measured. van't Hoff analysis was carried out (Fig. 6) for the reactions of **1** with **3a** (X = H), **3c** (X = OMe), and **3f** (X = CF_3). These particular silanes were chosen to represent a breadth of electronic character. The ΔS_{OA} values are all large and negative, reflecting the loss of entropy in this reaction between three reactants to form two products. ΔH_{OA} is negative for all three substrates, but more importantly, a clear trend is observed: **8f** < **8a** < **8c** (CF_3 < H < OMe) in ΔH_{OA}. These data show that the reaction between **1** and silanes **3** is more favourable with electron-poor silanes, which we interpret to mean that there is an increased strength of the Pd–Si bond in products **8**.[87]

To determine if this trend in the electronic influence of silanes is more general, we returned to triaryl silanes **5**. Because the equilibrium constants are too large to measure at room temperature under our standard conditions, we took advantage of the reaction's full reversibility in product distribution by performing competition experiments. In these experiments, 2.05 equivalents of each $HSiPh_3$ (**5a**) and $HSi(4\text{-X–Ph})_3$ (**5b–f**, X = NMe_2, OMe, Me, F, CF_3) were added to one equivalent of **1** (Fig. 7).

As with the non-competitive oxidative addition reactions of dimethylaryl silanes **3a–f** (Fig. 5), these data show that oxidative addition occurs preferentially with the more electron-poor silane. For example, when **5a** (a comparatively electron-neutral

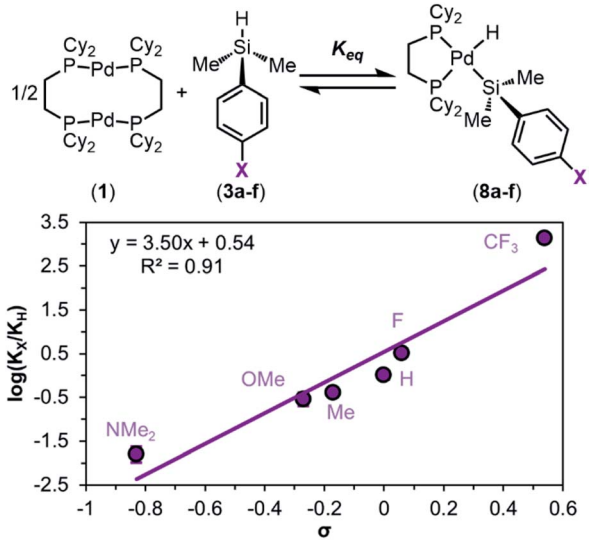

Fig. 5 Hammett plot of the equilibrium constants for the reaction between dimethylaryl silanes **3** and **1**. K_{eq} values were determined using the NMR integrations of each product. Reaction conditions: 1.00 equiv. of **1**, 2.05 equiv. of **3a–f**, 13.33 mM in C_6D_6 at 298 K.

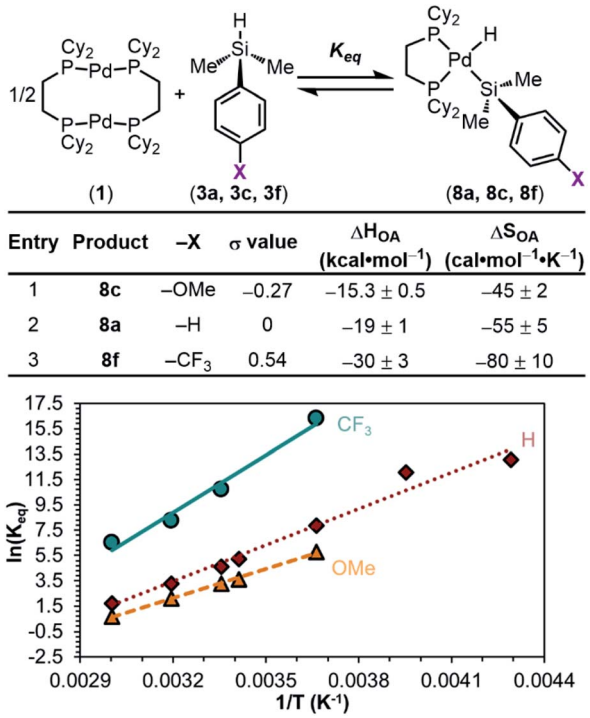

Entry	Product	–X	σ value	ΔH_{OA} (kcal•mol^{-1})	ΔS_{OA} (cal•mol^{-1}•K^{-1})
1	**8c**	–OMe	–0.27	–15.3 ± 0.5	–45 ± 2
2	**8a**	–H	0	–19 ± 1	–55 ± 5
3	**8f**	–CF_3	0.54	–30 ± 3	–80 ± 10

Fig. 6 van't Hoff analyses of the reaction equilibrium between dimethylaryl silanes **3** and **1**. Reaction conditions: 1.00 equiv. of 1, 2.05 equiv. of **3a**, **3c** or **3f**, 13.33 mM in C_7D_8, 253–333 K.

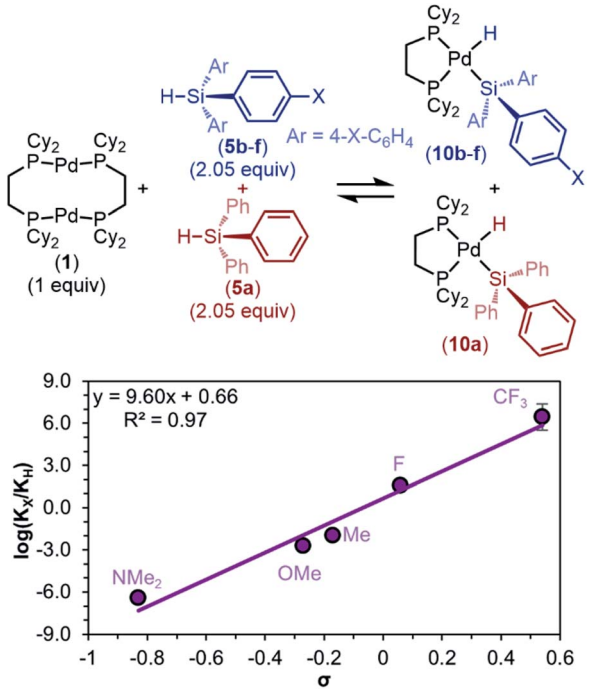

Fig. 7 Hammett plot of competition experiments between **5a** and electronically diverse silanes **5b–f** for oxidative addition with **1**. Reaction conditions: 1.00 equiv. of **1**, 2.05 equiv. of **5a** plus 2.05 equiv. of **5b–f**, 13.33 mM in C_6D_6, 298 K. Hammett plot constructed from K_{eq} values derived from conversions.

silane) and **5e** (an electron-poor silane) compete over the reaction with **1**, oxidative addition preferentially occurs with **5e** over **5a**, forming **10e** in larger concentrations than **10a**. Because the relative ratios of products are proportional to the ratios of equilibrium constants (see ESI Section 5b† for derivation), a Hammett plot was constructed to quantify the effect of electronic factors on the equilibrium constant of oxidative addition (Fig. 7). For triaryl silanes, Hammett analysis gives $\rho_{eq(comp)} = 9.6 \pm 0.9$, showing a more dramatic effect on K_{eq} than monoaryl silanes (non-competitive equilibrium data in Fig. 5, $\rho_{eq} = 3.5 \pm 0.5$). However, to allow for a direct comparison of the two systems, we additionally performed the same competition studies with dimethylaryl silanes **3a–f** (Table S18 and Fig. S16†). $\rho_{eq(comp)}$ was found to be 3.4 ± 0.3 with these dimethylaryl silanes. Notably, these data trend proportionally to the number of changing substituents at silicon.

To conclude studies on the reaction equilibrium, we sought to determine the effect of deuterium substitution in the silane. Reaction of **1** and **3a–d$_1$** proceeded as expected, affording product **8a–d$_1$**; the $^{31}P\{^1H\}$ NMR spectrum at room temperature shows a 1 : 1 : 1 triplet ($^2J_{D-P} = 11$ Hz) in 40% conversion. As with **3a**, the coupling constant is an average of the *cis* and *trans* coupling due to dynamic exchange behaviour (*vide infra*). The equilibrium constants for the reactions of proteo-silane **3a** and deutero-silane **3a–d$_1$** were determined independently (Table S11†). The equilibrium isotope effect (EIE) was determined to be 3.7 ± 0.2 at 298 K. The room temperature IR stretching frequencies for the Si–H and Si–D bonds in **3a** and **3a–d$_1$** are 2116 cm^{-1} and 1539 cm^{-1}, respectively. The EIE measured for this reaction is consistent with the fact that deuterium prefers to form the stronger bond;[94,110,111] *i.e.*, $K_{eq(D)}$ is lower than $K_{eq(H)}$ because the difference in energy between the Si–D and Pd–D bonds is larger than the difference in energy between the Si–H and Pd–H bonds.

Reaction kinetics

Having examined the ground state, we next turned our attention to understanding the kinetics and reaction mechanism. In probing the mechanism, three possible pathways for oxidative addition were considered: concerted, S_N2-like, or radical. A concerted pathway was deemed most reasonable as Si–H bonds are non-polar and have been shown to proceed *via* concerted pathways in related systems. We ruled out the S_N2-like pathway on the basis of relative acidities of Pd–H ($pK_a \approx 24$)[112] and Si–H ($pK_a \approx 35$)[113] bonds. Additionally, no by-products were observed that would result from a radical pathway (Si–Si bond coupling, H_2, *etc.*), so we shifted our attention from that pathway as well.

In line with a concerted pathway, the proposed mechanism for oxidative addition is seen in Fig. 8. *Step i* is dissociation of dimer **1** into monomers **12** in solution.[114] The 14-electron complex **12** can then react with silane in *step ii* to form σ-complex **13**, which then undergoes oxidative cleavage of the Si–H bond to form the product in *step iii*. These steps were taken as the basis for determination of the rate determining step (RDS) of the reaction.

If *step i* is rate-determining, then the rate law will show 0.5th order in **1**, 0th order in silane, and there will be no effect of electronic or deuterium substitution in the silane on the rate of the reaction ($\rho^{\ddagger} = 0$ for a Hammett plot and KIE = 1, respectively (KIE, kinetic isotope effect)). If *step ii* or *step iii* is the RDS, then the reaction will be 0.5th order in **1** and 1st order in silane; electron poor-silanes are expected to react faster ($\rho^{\ddagger} > 0$ in a Hammett plot); additionally, a normal, primary KIE is predicted. We expect that a small KIE would point toward *step ii* being the RDS, since the Si–H bond is only weakened in the transition state (**12** → **13**). A large, primary KIE would point toward *step iii* being the RDS, since it is during that step that the Si–H bond is cleaved.

Initial attempts to collect kinetic data by monitoring the reaction of **1** with **5a** by NMR proved unsuccessful, since the reaction was complete within a minute at room temperature. We thus set out to determine conditions that are amenable to reaction monitoring by NMR; however, even at low reagent concentrations (1.67 mM **1**, 3.42 mM **5a**) and low temperature (233 K), the formation of **10a** was too rapid to obtain reliable kinetic data. In line with our findings on reaction equilibria, we reasoned that Me_2PhSiH **3a** may also react more slowly in oxidative addition, yet still would have the advantage of allowing for electronic modulation *via* substitution on the aryl ring. Indeed, the gradual formation of a silyl palladium hydride **8a** is observable *via* $^{31}P\{^1H\}$ and ^1H NMR at 233 K.

As detailed above (Fig. 8), the rate law distinguishes between *step i* and *steps ii* or *iii* being the RDS; therefore, we first embarked on measuring the orders in the reactants. We utilized the method of initial rates to ensure that the rate of the backward reaction (from **8** to **1** and **3**) is negligible. Data was

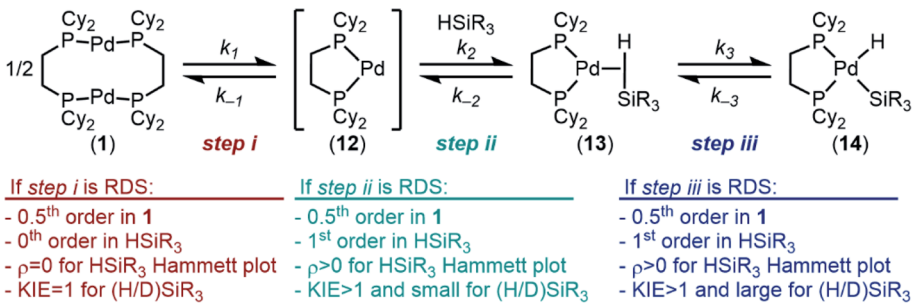

Fig. 8 Proposed mechanism for the oxidative addition of silanes to **1**.

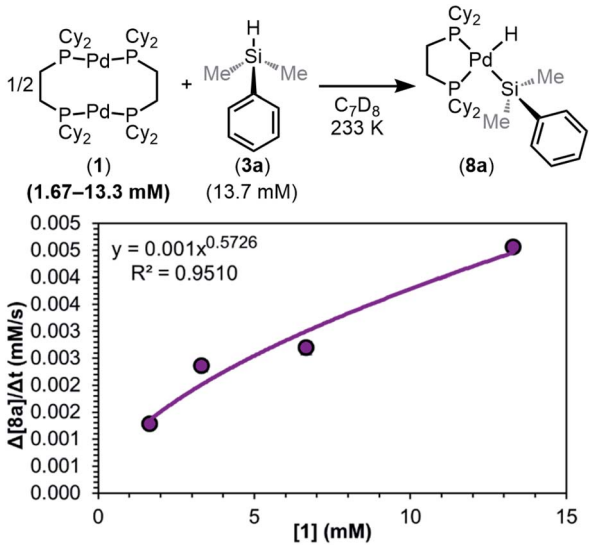

Fig. 9 Plot of initial rate *versus* [**1**]. Kinetics data was collected in C_7D_8 as the solvent at 233 K. Product concentration was determined by $^{31}P\{^1H\}$ NMR integration against an internal standard.

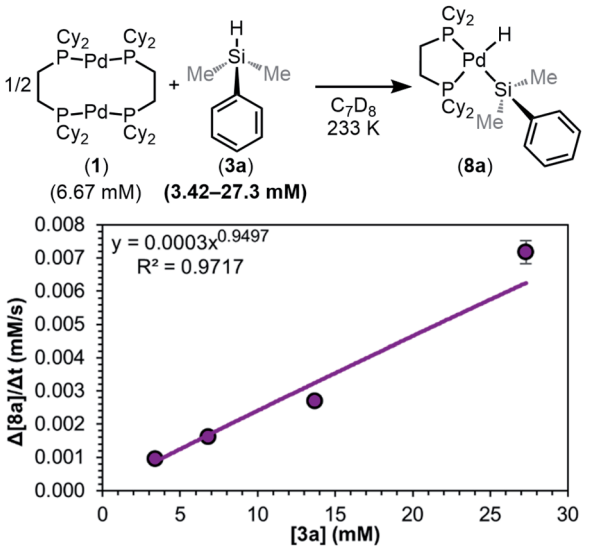

Fig. 10 Plot of initial rate *versus* [**3a**]. Kinetics data was collected in C_7D_8 as the solvent at 233 K. Product concentration was determined by $^{31}P\{^1H\}$ NMR integration against an internal standard.

collected on samples of varied concentrations of **1** (1.67–13.3 mM) or **3a** (3.42–27.3 mM) while the concentration of the unexamined reagent was kept constant. The observed rate of each reaction (Fig. S17 and S19†) was then plotted against initial reagent concentration to determine the reaction order.

As shown in Fig. 9, the reaction was determined to be 0.5^{th} order (0.57 ± 0.09) in dimer **1**. This result is consistent with any of the three steps in the mechanism of Fig. 8 being the RDS, and supports the hypothesis that the dimer **1** dissociates into two [(dcpe)Pd] fragments (**12**) prior to or during the RDS.

We next determined the order in silane (Fig. 10). A plot of the initial rate *versus* the concentration of **3a** shows that the reaction is 1^{st} order (0.9 ± 0.1) in silane. This suggests the silane is involved in or before the RDS, and thus dimer dissociation (*step i*) of the mechanism in Fig. 8 can be ruled out as the RDS. With these data, the simplified rate law of the reaction can be written (eqn (1)), showing an overall 1.5^{th} order reaction.

$$\text{Rate} = k_{obs}[\mathbf{1}]^{0.5}[\mathbf{3a}]^{1} \quad (1)$$

Having ruled out dimer dissociation as the RDS in the mechanism, we next examined the effect of electronic substitution at silicon on rates of reaction *via* a Hammett analysis. Rates of reaction were measured using dimethylaryl silanes **3a**, **3c**, and **3f**, and these experiments reveal a marked influence of silane electronics on the initial rates of product formation (Fig. S21–S24†). Analysis of kinetic trials for each silane gives a trend in k_{obs} of X = CF_3 > H > OMe, which follows the same trend as in equilibrium studies: strongly electron-withdrawing substituents at silicon favour rapid oxidative addition, while electron-donating substituents hinder the reaction rate.

A Hammett plot was constructed from these data (Fig. 11), which shows $\rho^{\ddagger} = 1.2 \pm 0.3$ (‡ notation is used to distinguish

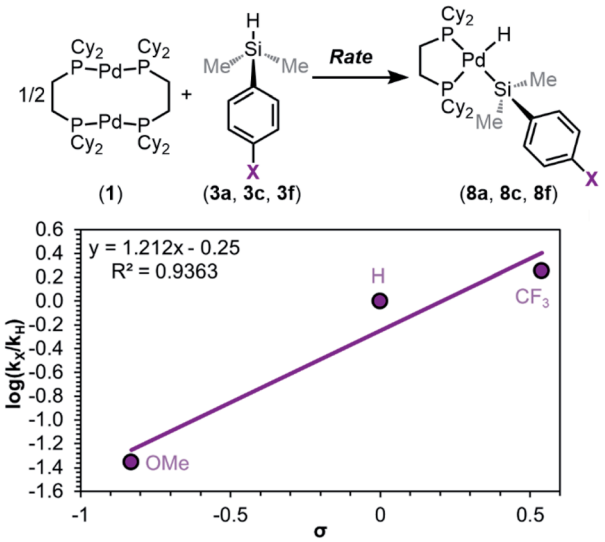

Fig. 11 Hammett plot constructed from kinetic data. Kinetic data was collected in C_7D_8 (13.33 mM) as the solvent at 233 K. Product concentration was determined by $^{31}P\{^1H\}$ NMR integration against an internal standard; 1.00 equiv. of **1** and 2.05 equiv. of **3a**, **3c**, or **3f** were used.

this sensitivity constant obtained from rates of reaction from the sensitivity constant obtained from reaction equilibrium constants (ρ_{eq})). Comparing the ρ value obtained for the reaction equilibrium ($\rho_{eq} = 3.5 \pm 0.5$) with that obtained for rates ($\rho^{\ddagger} = 1.2 \pm 0.3$) reveals that the observed rate of oxidative addition is approximately three times less sensitive to changes in electronics as the equilibrium constant (K_{eq}). The result of this Hammett analysis provides further evidence that either silane coordination (Fig. 8, *step ii*) or Si–H oxidative cleavage (Fig. 8, *step iii*) is the RDS of oxidative addition.

To help differentiate between these two steps being the RDS, the KIE of the reaction was determined. Recognizing the convoluted nature of KIEs and EIEs,[93,94,115,116] we continued using the method of initial rates to discount any equilibria involving reaction of the Si–H bond, and therefore measured rates of reaction are approximately independent of equilibrium effects. The initial rate of reaction for Me_2PhSiD (**3a–d$_1$**) was measured, and it was found to react more slowly than **3a**, with a KIE of 1.21 ± 0.04 (Fig. 12). The maximum primary KIE possible for Si–H/Si–D without invoking tunnelling is ~4 (see ESI, Section 9f† for details). Therefore, a KIE of 1.21 is large enough to be considered a primary isotope effect, but the magnitude is small and challenging to interpret. Either *step ii* is the RDS, in which a smaller magnitude KIE is rationalized by the Si–H bond not being formally broken in the transition state; or *step iii* is the RDS, in which a very early transition state (which is expected due to the high energy of the σ-complex) would lead to a lower magnitude KIE. Notably, the KIE reported here is consistent with those of other oxidative addition studies and catalytic reactions involving Si–H and C–H bond cleavage.[117]

We next sought to measure the barrier ($\Delta G^{\ddagger}_{OA}$) for the overall reaction by performing an Eyring analysis. The rate of reaction was measured as a function of temperature, and the results are seen in Fig. 13. $\Delta H^{\ddagger}_{OA}$ and $\Delta S^{\ddagger}_{OA}$ are obtained from the equation of the fit of the data, and as a result, $\Delta G^{\ddagger}_{OA}$ at a given temperature can be calculated. From the data in Fig. 13, $\Delta H^{\ddagger}_{OA}$ was determined to be 6.0 ± 0.3 kcal mol^{-1}, $\Delta S^{\ddagger}_{OA}$ was determined to be −40 ± 20 cal mol^{-1} K^{-1}, and therefore $\Delta G^{\ddagger}_{OA}$ at 233 K was calculated to be

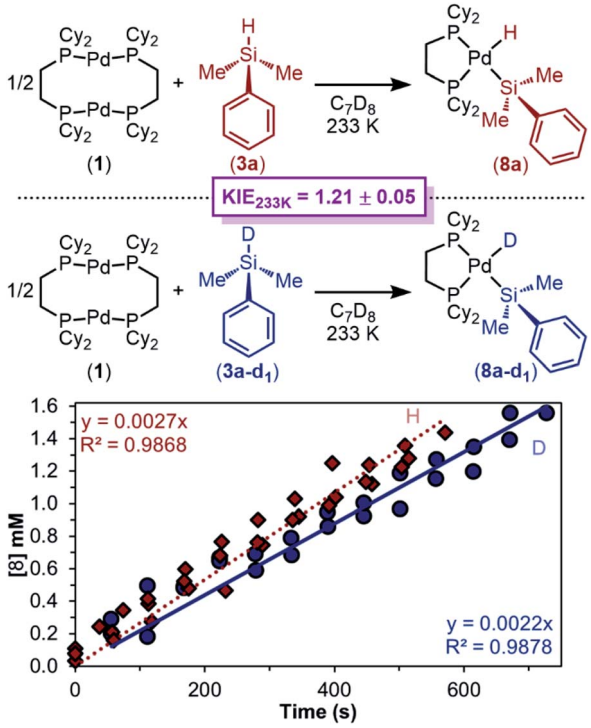

Fig. 12 Plot of [**8a**] or [**8a–d$_1$**] *versus* time. Kinetics data was collected in C_7D_8 (13.33 mM) as the solvent at 233 K. Product concentration was determined by $^{31}P\{^1H\}$ NMR integration against an internal standard; 1.00 equiv. of **1** and 2.05 equiv. of **3a** or **3a–d$_1$** were used.

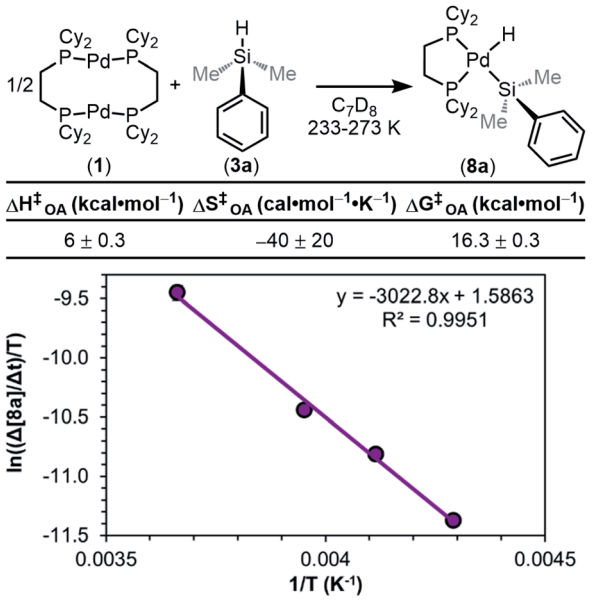

Fig. 13 Eyring plot constructed from variable temperature kinetics data in C_7D_8 (13.33 mM). Product concentration was determined by $^{31}P\{^1H\}$ NMR integration against an internal standard; 1.00 equiv. of **1** and 2.05 equiv. of **3a** was used. $\Delta G^{\ddagger}_{OA}$ determined at 233 K.

16.3 ± 0.3 kcal mol^{-1}. This large, negative value for $\Delta S^{\ddagger}_{OA}$ supports the proposed mechanism in Fig. 8. The transition state of the RDS is highly ordered relative to the ground state, consistent with *step ii* or *iii* being the RDS. These kinetic data have been compiled, and the observed rate constants (k_{obs}) have been determined using the rate law in eqn (1) (Table 1).

Dynamic exchange behaviour

One interesting feature of these silyl metal hydride complexes is their fluxional behaviour in solution.[33–35,118,119] We recognized

Table 1 Summary of rate constants (k_{obs}) obtained[a]

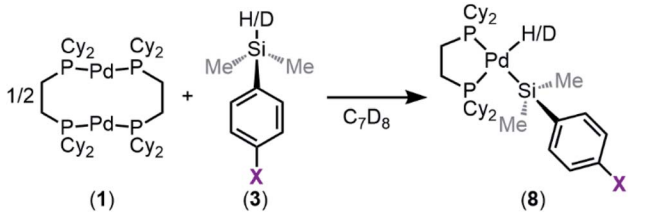

Entry	Pd complex	–H/D	–X	Temperature	k_{obs} (mM$^{0.5}$ s^{-1})
1	**8a**	–H	–H	233 K	9×10^{-5}
2	**8a**	–H	–H	243 K	1.4×10^{-4}
3	**8a**	–H	–H	253 K	2.1×10^{-4}
4	**8a**	–H	–H	273 K	5.9×10^{-4}
5	**8a-d$_1$**	–D	–H	233 K	3.2×10^{-4}
6	**8c**	–H	–OMe	233 K	3.3×10^{-6}
7	**8f**	–H	–CF_3	233 K	1.4×10^{-4}

[a] k_{obs} for the formation of **8a** at 233 K was determined from eight trials, and the value reported is the average (standard deviation is 1×10^{-5}).

that investigating this dynamic exchange (DE) behaviour would provide insight into the overall reaction mechanism of oxidative addition because it offers a unique chance to probe the oxidative cleavage and reductive coupling steps (k_3 and k_{-3}, respectively, in Fig. 8) independent of the overall oxidative addition process. Accordingly, solution ^{1}H and ^{31}P{^{1}H} NMR spectra of product **8a** were recorded at multiple temperatures (Fig. 14). At very low temperatures, the ^{31}P{^{1}H} NMR spectrum shows two singlets (δ 58.4 and 57.4 ppm at 183 K) which undergo coalescence at 213 K, eventually forming a sharp singlet (δ 56.4 ppm at 273 K (Fig. 14a). Similar behaviour is seen for the Pd–H peak in the ^{1}H NMR spectra at low temperatures; a doublet of doublets (δ −1.39 ppm, $^2J_{\mathrm{H-P}(trans)} = 192.6$ Hz, $^2J_{\mathrm{H-P}(cis)} = 7.9$ Hz at 183 K) proceeds through coalescence at 213 K to eventually form an apparent triplet, centring at −1.71 ppm, $^2J_{\mathrm{H-P}} = 75.4$ Hz at 273 K) (Fig. 14b). Line broadening analysis[120,121] allows for the calculation of the barriers for this dynamic exchange (DE) process. $\Delta H^{\ddagger}_{\mathrm{DE}}$, $\Delta S^{\ddagger}_{\mathrm{DE}}$, and $\Delta G^{\ddagger}_{\mathrm{DE}}$ at 233 K were determined to be 7.7 ± 0.4 kcal mol^{-1}, −10.7 ± 0.5 cal mol^{-1} K, and 10.2 ± 0.4 kcal mol^{-1}, respectively.

In analogy to reported complexes and their dynamic exchange behaviour,[61,82–84] we propose a mechanism in Scheme 2 that accounts for these NMR spectra. **8a** and **8a′** are proposed to interconvert *via* the σ-complexes **13a** and **13a′**, which themselves interconvert by rotation around the Pd–(η^2-H–SiMe$_2$Ph) bond (k_4 and k_{-4}). Conversion of **8a** into **13a** and **8a′** into **13a′** are reductive coupling steps (k_{-3}), the microscopic reverse of oxidative cleavage (k_3).

At elevated temperatures, exchange is rapid on the NMR timescale, and the Pd–H signal in the ^{1}H NMR appears as a triplet due to coupling to both P nuclei, and the coupling constant is an average of the *trans* and the *cis* $^2J_{\mathrm{H-P}}$ values. This

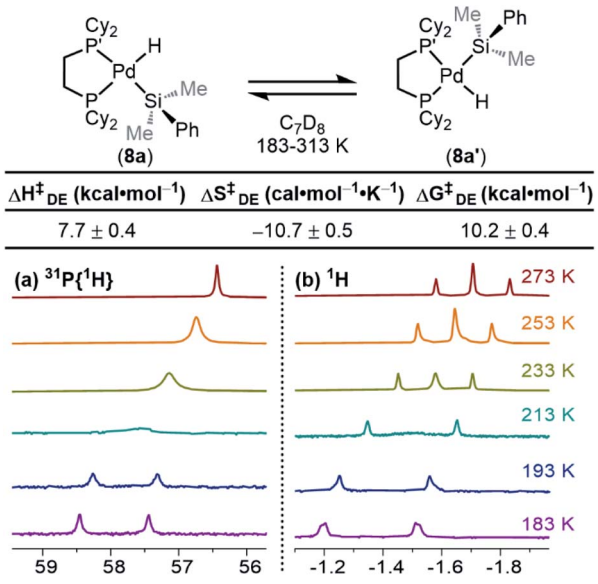

Fig. 14 (a) ^{31}P{^{1}H} NMR spectra and (b) ^{1}H NMR spectra of the Pd–H region of **8a**/**8a′** as a function of temperature with the measured barriers for dynamic exchange (DE). Spectra collected in C_7D_8 (13.33 mM). $\Delta G^{\ddagger}_{\mathrm{DE}}$ determined at 233 K.

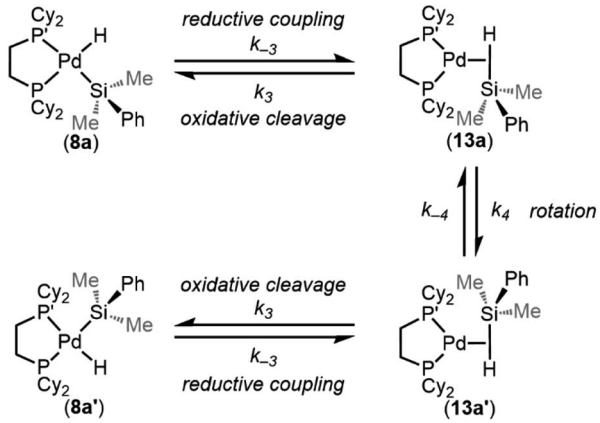

Scheme 2 Proposed mechanism for the intramolecular dynamic exchange of –H and –SiMe$_2$Ph environments.

interpretation is supported by the ^{31}P{^{1}H} NMR data, which shows a singlet at elevated temperatures. Upon cooling, the Pd–H signal (^{1}H NMR) undergoes coalescence and gradually resolves into a doublet of doublets at sufficiently low temperatures. The splitting pattern is accounted for by the inequivalency of the P nuclei; at low temperature in the ^{31}P{^{1}H} NMR, two distinct phosphorous environments are observed, as exchange is sufficiently slowed and both P nuclei environments (P and P′ in Scheme 2) are discrete. The tunability of this process from slow-exchange to fast-exchange over an accessible temperature range indicates a relatively small energy barrier for conversion between species, and is consistent with the measured barrier of 10.2 ± 0.4 kcal mol^{-1} at 233 K.

Important for the overall oxidative addition reaction (formation of **8a** from **1** and **3a**), the RDS of this dynamic exchange process is either the barrier for reductive coupling/oxidative cleavage (k_{-3}/k_3) or the barrier for rotation (k_4/k_{-4}). Therefore, the oxidative cleavage step (k_3) must be equal to or less than 10.2 ± 0.4 kcal mol^{-1} at 233 K.

Taking advantage of the line broadening observed for additional silyl palladium hydrides, we sought to investigate the effect of silane substitution on the barriers for DE. We focused on triaryl silanes **5** because not all products with dimethylaryl silanes **3** reached the slow exchange regime at temperatures accessible in toluene-d_8. The activation parameters (Table 2) show that there is no significant effect of electronic or isotopic substitution on the rate of dynamic exchange for triaryl silanes since the measured barriers are mostly within error of one another. $\Delta H^{\ddagger}$ varies from 10–14 kcal mol^{-1}, showing a trend of more electron-poor silanes having higher enthalpic barriers than electron-rich silanes, and $\Delta S^{\ddagger}$ is close to zero. In this dynamic exchange process, $\Delta H^{\ddagger}$ and $\Delta S^{\ddagger}$ are opposing, and $\Delta G^{\ddagger}$ for products **10a**, **10c**, and **10f** are within error of one another, resulting in a net null electronic effect. Furthermore, the barriers for this dynamic exchange process for **10a–d$_1$** and **10a** are also within error, implying a KIE of approximately 1 (within error). Measuring the rates of dynamic exchange at varying concentrations of **10f** gave similar values; these data along with small values of $\Delta S^{\ddagger}$ support our hypothesis that the process is

Table 2 Dynamic exchange (DE) barriers determined by linewidth analysis of $^{31}P\{^1H\}$ NMR spectra at variable temperature. $\Delta H^{\ddagger}_{DE}$ and $\Delta G^{\ddagger}_{DE}$ are reported in kcal mol^{-1} and $\Delta S^{\ddagger}_{DE}$ is reported in cal mol^{-1} K^{-1}. $\Delta G^{\ddagger}_{DE}$ determined at 233 K

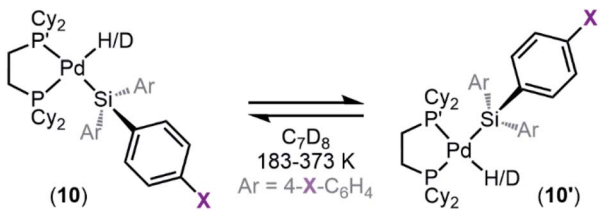

Entry	Pd complex	–H/D	–X	$\Delta H^{\ddagger}_{DE}$	$\Delta S^{\ddagger}_{DE}$	$\Delta G^{\ddagger}_{DE}$
1	**10a**	–H	–H	12 + 1	3.5 + 0.3	11 + 1
2	**10a-d$_1$**	–D	–H	10.0 + 0.4	−2.46 + 0.09	10.6 + 0.4
3	**10c**	–H	–OMe	10.1 + 0.4	−2.80 + 0.09	10.7 ± 0.4
4	**10f**	–H	–CF$_3$	13.7 + 0.5	5.5 ± 0.2	12.5 ± 0.5

intramolecular. These results point toward rotation (k_4, Scheme 2) being the RDS of dynamic exchange since, if reductive coupling/oxidative cleavage were the RDS, a measurable electronic effect and KIE would be expected. Notably, this conclusion has also been drawn for silyl-Rh complexes,[61] and values are similar to known dynamic exchange processes of silyl Ni, Pd, Pt, and Rh complexes.[46,61,82,92]

Constructing a reaction coordinate diagram

Taking our findings from equilibrium and kinetic studies, we have constructed a complete mechanistic picture for the oxidative addition of silanes to **1**. With the bulk of the data obtained using dimethylphenyl silane **3a**, we focus on those results in the discussion below (Fig. 15), but we expect the general trends to be analogous for the other silanes studied in this work.

ΔG_{OA} was determined in the course of studying the reaction equilibrium. K_{eq} for the reaction between **3a** and **1** at 233 K was determined to be 125, corresponding to $\Delta G_{OA} = -6 \pm 1$ kcal mol^{-1} (Fig. 15, purple). Therefore, the silyl palladium hydride **8a** is lower in energy by 6 kcal mol^{-1} than the starting materials **1** and **3a**. This energy difference is larger for electron-poor silanes than electron-rich silanes, as shown *via* Hammett plots (Fig. 5, 7 and S16†).

The reaction was found to be 1st order in silane **3a** (Fig. 10) and 0.5th order in palladium dimer **1** (Fig. 9). Because there is a dependence on the silane on the rate of reaction, dimer dissociation (**1** → **12**) is ruled out as the RDS. Therefore, either formation of the σ-complex **13a** or oxidative cleavage of the Si–H bond must be the RDS, since both would account for the observed orders in reactants. Hammett analysis of the dependence of the rate of reaction on the electronic influence of the silane (Fig. 11) also does not differentiate between σ-complex formation and oxidative cleavage being the RDS, since the barriers for both steps are expected to be lowered with electron-poor silanes, in line with the observed trends. Based on the small, but primary KIE of 1.21 ± 0.04 (Fig. 12), we hypothesized that formation of the σ-complex **13a** is the RDS, since cleavage of the Si–H bond is expected to result in a larger KIE value. However, this is not definitive evidence.

The reaction barrier for the full oxidative addition process (**1** + **3a** → **8a**) was determined to be 16.3 ± 0.3 kcal mol^{-1} by an Eyring analysis (Fig. 13). By linewidth analysis of the $^{31}P\{^1H\}$ NMR spectra of product **8a**, we determined that the barrier for the dynamic exchange process between **8a** and **8a**′ *via* **13a**/**13a**′ is 10.2 ± 0.4 kcal mol^{-1} (Fig. 14). Because no significant KIE or electronic effect was observed for the dynamic exchange process, we concluded that the RDS of dynamic exchange is likely rotation. Therefore, the maximum barrier of reductive coupling (the microscopic reverse of oxidative cleavage, or **8a** → **13a**) is equal to or lower than 10 kcal mol^{-1}. If oxidative cleavage (**13a** → **8a**) was the RDS, then the maximum overall reaction barrier for oxidative addition would be the sum of ΔG_{OA} (−6 ± 1 kcal mol^{-1}) and $\Delta G^{\ddagger}_{DE}$ (10.2 ± 0.4 kcal mol^{-1}). This sum (4 kcal mol^{-1}) is much less than the measured free energy barrier for oxidative addition (16.3 ± 0.3 kcal mol^{-1}). Therefore, formation of the σ-complex (*step ii* in Fig. 8) is deduced to be the RDS. As a consequence of *step ii* being the RDS, equilibria involving the silane and reaction of the Si–D/H bond are not included in the rate law, and the KIE can be considered separately from the EIE. Because of the importance in oxidative addition reactions in catalysis, we expect these findings to affect the design of silanes and catalysts for many catalytic reactions.

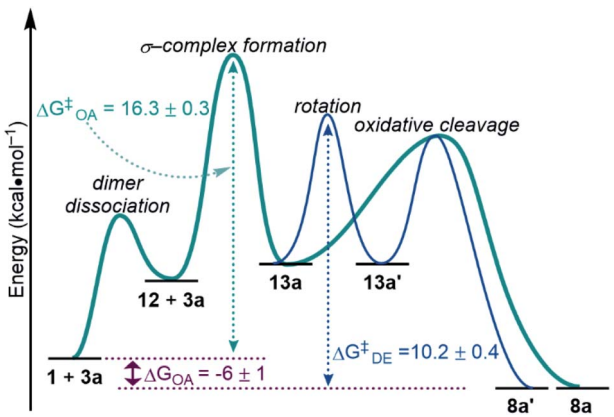

Fig. 15 Reaction coordinate diagram with experimentally determined free energy values at 233 K. OA, oxidative addition. DE, dynamic exchange.

Application to catalysis

Having fully elucidated the mechanism of the oxidative addition of silanes to palladium(0), we next demonstrate the relevance of this work to catalysis. Hydrosilylation was our first target because of its importance and industrial relevance. Subjecting complex **1** to $HSiPh_3$ (**5a**) and phenylacetylene (**15**) in toluene resulted in 66% yield of hydrosilylation products. Two regioisomers were observed: the branched product (α-**16a**) and the linear *E*-alkene (*E*-β-**16a**) in a 1 : 8 ratio. These results are consistent with related Pd(0)-catalysed hydrosilylation

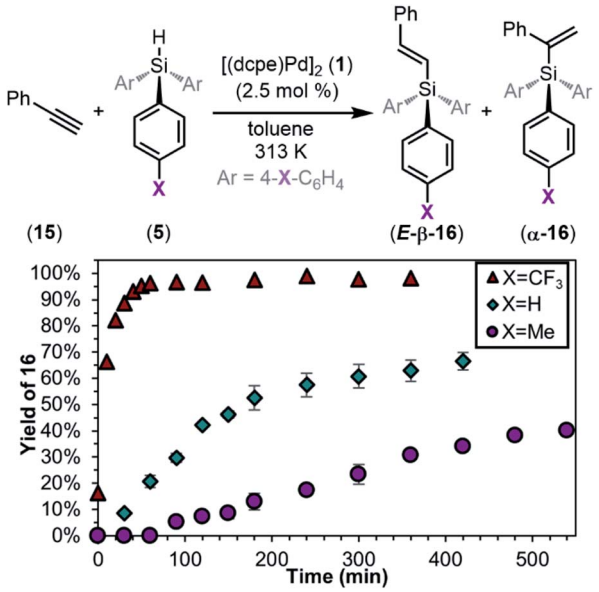

Fig. 16 1-Catalysed hydrosilylation of phenylacetylene and silanes **5**. Reaction conditions: **15** (1 equiv.), **5** (1 equiv.), **1** (2.5 mol%), 0.04 M in toluene, 313 K. Yields are the sum of the yields of both products (*E*-β-**16** + α-**16**) determined by GCMS using a calibration curve against 1,3,5-trimethoxybenzene. Selectivities of *E*-β-**16** + α-**16** are as follows: *E*-β-**16f**/α-**16f** = 34 : 1 (X = CF_3); *E*-β-**16a**/α-**16a** = 8 : 1 (X = H); *E*-β-**16d**/α-**16d** = 6 : 1 (X = Me).

reactions.[122,123] Notably, the effect of silane electronics on alkyne hydrosilylation has not been investigated in the literature. When compared to the neutral silane **5a**, the rate of the reaction is faster with the electron-poor silane **5f** and slower with the electron-rich silane **5d** (Fig. 16). Reaction with **5f** gives products α-**16f** and *E*-β-**16f** in 98% yield in a 1 : 34 ratio, and reaction with **5d** gives products α-**16d** and *E*-β-**16d** in 40% yield in a 1 : 6 ratio. These results directly parallel the data obtained from oxidative addition and highlight the importance of studying this fundamental reaction in organometallic chemistry. Furthermore, using the isolated complex **10a** as a catalyst in 5 mol% leads to a reaction profile nearly identical to that generated from **1**/**5a** mixtures (see ESI Section 11†), further supporting the relevance of this oxidative addition to catalysis.

Conclusions

In this work, we have elucidated the mechanism of oxidative addition of Pd(0) to Si–H bonds and shown the relevance of this reaction in catalytic hydrosilylation. We evaluated the impact of silane electronic influence in the oxidative addition of $[(\mu\text{-dcpe})Pd]_2$ to form well-defined, mononuclear silyl palladium hydrides. A library of electronically varied silanes have been synthesized and the corresponding silyl palladium hydrides characterized, including *via* single crystal diffraction of **10f**. Extensive equilibrium and competition studies point to a pronounced effect of silane electronics in the oxidative addition reaction, quantified *via* Hammett analysis to show the reaction with triaryl silanes **5** to be approximately three times more sensitive to electronics than with dimethylaryl silanes **3**. Formation of (silyl)Pt(H) and (silyl)Rh(H) complexes *via* silane oxidative addition have shown a similar trend of being more favourable with electron-withdrawing substituents at silicon.[44,49,61] van't Hoff analysis suggests that this trend arises from the corresponding Pd–Si bond strength in products **10** and **8**. Our conclusion that Pd–Si bond strength is related to the identity of the silicon substituents is supported by computational work of related Pd complexes.[87] The formed silyl palladium hydrides exist in a dynamic equilibrium with **1** that is fully reversible with regard to both temperature and product distribution, which is similar to behaviour of (silyl)Pt(H) complexes.[50] Kinetic studies further support the favourability of electron-poor silanes and show that the rate of reaction (k_{obs}) is less sensitive to electronics than the equilibrium constant (K_{eq}).

Further, this system is well-suited to answer long-standing questions in the oxidative addition of palladium to hydrosilanes *via* mechanism elucidation. The reaction is 0.5th order in starting dimer **1** and 1st order in silanes. The reaction barrier was determined to be 16.3 kcal mol^{-1} using Eyring analysis. This energy barrier far exceeds that of oxidative cleavage of the Si–H bond, (determined to be equal to or less than 10 kcal mol^{-1}). The upper limit of the barrier for oxidative cleavage was determined by studying the dynamic behaviour of the (silyl)Pd(H) complexes on the NMR timescale. Analogous behaviour has been observed with (silyl)Pt(H) complexes, which was shown to be an intramolecular process involving reductive coupling of the hydride and silyl ligands.[59,61,124,125] The barriers for dynamic exchange of these Pt complexes are approximately the same as the barriers reported here for (silyl)Pd(H) complexes.[61] In conjunction with a small, primary KIE, we conclude that the RDS of oxidative addition is the formation of the σ-complex, not Si–H bond cleavage.

Lastly, we showed the relevance of our findings to catalysis, namely hydrosilylation. Electronic variation of the silane in catalysis directly parallels that of oxidative addition, which further supports the relevance and importance of in-depth mechanistic studies to catalysis.

Data availability

All data collected for this article, including experimental procedures, compound characterization, conversion values and graphical data, and NMR and IR spectra are available in the ESI.†

Author contributions

M. R. H. and A. K. C. are responsible for conceptualization, investigation, and manuscript writing. M. R. H. carried out all experimentation except crystallography. L. N. Z. performed all crystallography experimentation, data collection, and analysis. A. K. C. is responsible for supervision and project administration. All authors edited and reviewed the manuscript.

Conflicts of interest

There are no conflicts to declare.

Acknowledgements

This research was supported by the Energy and Sustainable Materials Cluster and the Office of the Vice President of Research at the University of Oregon. The authors would like to acknowledge contributions from Dr Nanette Jarenwattanon (NMR experiment preparation and analysis).

Notes and references

1 V. V. Grushin, Hydrido Complexes of Palladium, *Chem. Rev.*, 1996, **96**, 2011–2034.
2 K. K. M. Hii, in *Handbook of Organopalladium Chemistry for Organic Synthesis*, ed. N. Ei-ichi, 2003, pp. 81–90.
3 R. F. Heck, Palladium-catalyzed reactions of organic halides with olefins, *Acc. Chem. Res.*, 1979, **12**, 146–151.
4 I. P. Beletskaya and A. V. Cheprakov, The Heck Reaction as a Sharpening Stone of Palladium Catalysis, *Chem. Rev.*, 2000, **100**, 3009–3066.
5 I. D. Hills and G. C. Fu, Elucidating Reactivity Differences in Palladium-Catalyzed Coupling Processes: The Chemistry of Palladium Hydrides, *J. Am. Chem. Soc.*, 2004, **126**, 13178–13179.
6 M. S. Sigman and D. R. Jensen, Ligand-Modulated Palladium-Catalyzed Aerobic Alcohol Oxidations, *Acc. Chem. Res.*, 2006, **39**, 221–229.
7 D. Wang, A. B. Weinstein, P. B. White and S. S. Stahl, Ligand-Promoted Palladium-Catalyzed Aerobic Oxidation Reactions, *Chem. Rev.*, 2018, **118**, 2636–2679.
8 S. E. Mann, L. Benhamou and T. D. Sheppard, Palladium(II)-Catalysed Oxidation of Alkenes, *Synthesis*, 2015, **47**, 3079–3117.
9 J. F. Hartwig, *Organotransition Metal Chemistry: From Bonding to Catalysis*, University Science, 2010.
10 G. Cavinato and L. Toniolo, Carbonylation of Ethene Catalysed by Pd(II)-Phosphine Complexes, *Molecules*, 2014, **19**, 15116–15161.
11 Z. Chen and M. Brookhart, Exploring Ethylene/Polar Vinyl Monomer Copolymerizations Using Ni and Pd α-Diimine Catalysts, *Acc. Chem. Res.*, 2018, **51**, 1831–1839.
12 E. Larionov, H. Li and C. Mazet, Well-defined transition metal hydrides in catalytic isomerizations, *Chem. Commun.*, 2014, **50**, 9816–9826.
13 J. J. Molloy, T. Morack and R. Gilmour, Positional and Geometrical Isomerisation of Alkenes: The Pinnacle of Atom Economy, *Angew. Chem., Int. Ed.*, 2019, **58**, 13654–13664.
14 B. M. Trost, Palladium-catalyzed cycloisomerizations of enynes and related reactions, *Acc. Chem. Res.*, 1990, **23**, 34–42.
15 H.-H. Moretto, M. Schulze and G. Wagner, in *Ullmann's Encyclopedia of Industrial Chemistry*, 2012.
16 R. Y. Lukin, A. M. Kuchkaev, A. V. Sukhov, G. E. Bekmukhamedov and D. G. Yakhvarov, Platinum-Catalyzed Hydrosilylation in Polymer Chemistry, *Polymers*, 2020, **12**, 2174.
17 S. B. J. Kan, R. D. Lewis, K. Chen and F. H. Arnold, Directed evolution of cytochrome c for carbon–silicon bond formation: Bringing silicon to life, *Science*, 2016, **354**, 1048–1051.
18 A. K. Franz and S. O. Wilson, Organosilicon Molecules with Medicinal Applications, *J. Med. Chem.*, 2013, **56**, 388–405.
19 E. Rémond, C. Martin, J. Martinez and F. Cavelier, Silicon-Containing Amino Acids: Synthetic Aspects, Conformational Studies, and Applications to Bioactive Peptides, *Chem. Rev.*, 2016, **116**, 11654–11684.
20 G. A. Showell and J. S. Mills, Chemistry challenges in lead optimization: silicon isosteres in drug discovery, *Drug Discovery Today*, 2003, **8**, 551–556.
21 B. Marciniec, *Hydrosilylation*, Springer, 2009.
22 B. Marciniec, Catalysis by transition metal complexes of alkene silylation–recent progress and mechanistic implications, *Coord. Chem. Rev.*, 2005, **249**, 2374–2390.
23 D. Troegel and J. Stohrer, Recent advances and actual challenges in late transition metal catalyzed hydrosilylation of olefins from an industrial point of view, *Coord. Chem. Rev.*, 2011, **255**, 1440–1459.
24 Y. Nakajima and S. Shimada, Hydrosilylation reaction of olefins: recent advances and perspectives, *RSC Adv.*, 2015, **5**, 20603–20616.
25 A. K. Roy, A Review of Recent Progress in Catalyzed Homogeneous Hydrosilation (Hydrosilylation), *Adv. Organomet. Chem.*, 2007, **55**, 1–59.
26 T. K. Meister, K. Riener, P. Gigler, J. Stohrer, W. A. Herrmann and F. E. Kühn, Platinum Catalysis Revisited—Unraveling Principles of Catalytic Olefin Hydrosilylation, *ACS Catal.*, 2016, **6**, 1274–1284.
27 K. A. Horn, Regio- and Stereochemical Aspects of the Palladium-Catalyzed Reactions of Silanes, *Chem. Rev.*, 1995, **95**, 1317–1350.
28 M. Zaranek and P. Pawluc, Markovnikov Hydrosilylation of Alkenes: How an Oddity Becomes the Goal, *ACS Catal.*, 2018, **8**, 9865–9876.
29 T. Hayashi, Chiral Monodentate Phosphine Ligand MOP for Transition-Metal-Catalyzed Asymmetric Reactions, *Acc. Chem. Res.*, 2000, **33**, 354–362.
30 S. E. Gibson and M. Rudd, The Role of Secondary Interactions in the Asymmetric Palladium-Catalysed Hydrosilylation of Olefins with Monophosphane Ligands, *Adv. Synth. Catal.*, 2007, **349**, 781–795.
31 J. W. Han and T. Hayashi, Palladium-catalyzed asymmetric hydrosilylation of styrenes with trichlorosilane, *Tetrahedron: Asymmetry*, 2014, **25**, 479–484.
32 L. F. Tietze, H. Ila and H. P. Bell, Enantioselective Palladium-Catalyzed Transformations, *Chem. Rev.*, 2004, **104**, 3453–3516.
33 J. Y. Corey and J. Braddock-Wilking, Reactions of Hydrosilanes with Transition-Metal Complexes: Formation of Stable Transition-Metal Silyl Compounds, *Chem. Rev.*, 1999, **99**, 175–292.
34 J. Y. Corey, Reactions of Hydrosilanes with Transition Metal Complexes and Characterization of the Products, *Chem. Rev.*, 2011, **111**, 863–1071.

35 J. Y. Corey, Reactions of Hydrosilanes with Transition Metal Complexes, *Chem. Rev.*, 2016, **116**, 11291–11435.
36 F. de Charentenay, J. A. Osborn and G. Wilkinson, Interaction of silanes with tris(triphenylphosphine) chlororhodium(I) and other rhodium complexes; hydrosilation of hex-1-ene by use of trichlorosilane, *J. Turk. Chem. Soc., Sect. A*, 1968, 787–790.
37 R. N. Haszeldine, R. V. Parish and D. J. Parry, Organosilicon chemistry. Part V. Rhodium(III)–silyl complexes and the hydrosilation of hex-1-ene, *J. Chem. Soc. A*, 1969, 683–690.
38 M. J. Fernandez, P. M. Bailey, P. O. Bentz, J. S. Ricci, T. F. Koetzle and P. M. Maitlis, Synthesis, x-ray, and low-temperature neutron-diffraction study of a rhodium(V) complex: dihydridobis(triethylsilyl)(pentamethylcyclopentadienyl) rhodium, *J. Am. Chem. Soc.*, 1984, **106**, 5458–5463.
39 M. Brockmann, H. t. Dieck and J. Klaus, Rhodium(I)-mono- und -diazadienkomplexe, synthese, spektroskopische charakterisierung, oxidative additionsreaktionen und einsatz in der homogenen katalyse zur hydrosilylierung, *J. Organomet. Chem.*, 1986, **301**, 209–226.
40 J. Ruiz, P. O. Bentz, B. E. Mann, C. M. Spencer, B. F. Taylor and P. M. Maitlis, The formation and characterisation of (η2-ethene)hydrido(η5-pentamethylcyclopentadienyl)(trisubstituted-silyl)rhodium complexes; intermediates in catalytic dehydrogenative silylation reactions, *J. Chem. Soc., Dalton Trans.*, 1987, 2709–2713.
41 S. B. Duckett, D. M. Haddleton, S. A. Jackson, R. N. Perutz, M. Poliakoff and R. K. Upmacis, Photochemical oxidative addition reactions of (.eta.5-cyclopentadienyl)bis(ethene) rhodium with dihydrogen and trialkylsilanes: formation and isolation of rhodium(III) and rhodium(V) hydrides, *Organometallics*, 1988, **7**, 1526–1532.
42 D. P. Drolet and A. J. Lees, Solution photochemistry of (.eta.5-C5R5)Rh(CO)2 (R = H, Me) complexes: pathways for photosubstitution and C-H/Si-H bond activation reactions, *J. Am. Chem. Soc.*, 1992, **114**, 4186–4194.
43 M. Aizenberg and D. Milstein, Catalytic Activation of Carbon-Fluorine Bonds by a Soluble Transition Metal Complex, *Science*, 1994, **265**, 359–361.
44 K. Osakada, S. Sarai, T.-a. Koizumi and T. Yamamoto, Structure and Chemical Properties of Chlorohydrido(diarylsilyl)rhodium(III) Complexes, mer-RhCl(H)(SiHAr2)(PMe3)3. Thermally Induced Chloro Transfer from Rhodium to Silicon in the Complexes and Silane Exchange, *Organometallics*, 1997, **16**, 3973–3980.
45 M. Okazaki, S. Ohshitanai, H. Tobita and H. Ogino, Synthesis, structure, and reactivity of {(2-phosphinoethyl) silyl}rhodium(i) complexes Rh[(κ2Si,P)-Me2Si(CH2) 2PPh2](PMe3)n (n = 2, 3), *J. Chem. Soc., Dalton Trans.*, 2002, 2061–2068.
46 K. A. M. Ampt, S. B. Duckett and R. N. Perutz, Photochemical reactions of (η5-cyclopentadienyl)bis(t-butylacrylate) rhodium with silanes: Dynamics of isomer interconversion via Rh(η2-silane) species, *Dalton Trans.*, 2004, 3331–3337.
47 E. Calimano and T. D. Tilley, Synthesis and reactivity of rhodium and iridium alkene, alkyl and silyl complexes supported by a phenyl-substituted PNP pincer ligand, *Dalton Trans.*, 2010, **39**, 9250–9263.
48 M. A. Esteruelas, M. Oliván and A. Vélez, POP-Pincer Silyl Complexes of Group 9: Rhodium versus Iridium, *Inorg. Chem.*, 2013, **52**, 12108–12119.
49 H. C. Clark and M. J. Hampden-Smith, Ligand Interactioins in crowded molecules, *Coord. Chem. Rev.*, 1987, **79**, 229–255.
50 C. Eaborn, B. Ratcliff and A. Pidcock, The preparation of hydrido(silyl)bis(triphenylphosphine)platinum(II) complexes from bis(triphenylphosphine)platinum-ethylene and silicon hydrides, *J. Organomet. Chem.*, 1974, **65**, 181–186.
51 E. A. V. Ebsworth, V. M. Marganian, F. J. S. Reed and R. O. Gould, Platinum hydrides containing silyl or germyl ligands. Crystal structure of trans-hydridosilylbis(tricyclohexylphosphine)platinum(II), *J. Chem. Soc., Dalton Trans.*, 1978, 1167–1170.
52 R. S. Paonessa, A. L. Prignano and W. C. Trogler, Photochemical generation of bis(phosphine)palladium and bis(phosphine)platinum equivalents, *Organometallics*, 1985, **4**, 647–657.
53 D. L. Packett, A. Syed and W. C. Trogler, Associative reactions of dihydridobis(trimethylphosphine) platinum(II). Molecular structures of (diphenylacetylene) bis(trimethylphosphine)platinum and hydridotris(trimethylphosphine)platinum(II) tetraphenylborate, *Organometallics*, 1988, **7**, 159–166.
54 D. F. Mullica, E. L. Sappenfield and M. J. Hampden-Smith, Synthesis and X-ray structural investigation of cis-hydrido(triphenylsilyl)-1,4-butanediyl-bis-(dicyclohexylphosphine)platinum(II), *Polyhedron*, 1991, **10**, 867–872.
55 L. D. Boardman, (.eta.5-Cyclopentadienyl)trialkylplatinum photohydrosilylation catalysts. Mechanism of active catalyst formation and preparation of a novel bis(silyl) platinum hydride, *Organometallics*, 1992, **11**, 4194–4201.
56 S. D. Grumbine, T. D. Tilley, F. P. Arnold and A. L. Rheingold, A Fischer-type silylene complex of platinum: [trans-(Cy3P)2(H)Pt:Si(SEt)2]BPh4, *J. Am. Chem. Soc.*, 1993, **115**, 7884–7885.
57 L. A. Latif, C. Eaborn, A. P. Pidcock and N. S. Weng, Square planar platinum(II) complexes. Crystal structures of cis-bis(triphenylphosphine)hydro (triphenylstannyl) platinum(II) and cis-bis(triphenylphosphine) hydro(triphenylsilyl)platinum(II), *J. Organomet. Chem.*, 1994, **474**, 217–221.
58 T.-a. Koizumi, K. Osakada and T. Yamamoto, Intermolecular Transfer of Triarylsilane from RhCl(H)(SiAr3)[P(i-Pr)3]2 to a Platinum(0) Complex, Giving cis-PtH(SiAr3)(PEt3)2 (Ar = C6H5, C6H4F-p, C6H4Cl-p), *Organometallics*, 1997, **16**, 6014–6016.
59 J. D. Feldman, G. P. Mitchell, J.-O. Nolte and T. D. Tilley, Isolation and Characterization of Neutral Platinum Silylene Complexes of the Type (R3P)2PtSiMes2 (Mes =

2,4,6-Trimethylphenyl), *J. Am. Chem. Soc.*, 1998, **120**, 11184–11185.

60 R. S. Simons, L. M. Sanow, K. J. Galat, C. A. Tessier and W. J. Youngs, Synthesis and Structural Characterization of the Mono(silyl)platinum(II) Complex cis-(2,6-Mes2C6H3(H)2Si)Pt(H)(PPr3)2, *Organometallics*, 2000, **19**, 3994–3996.

61 D. Chan, S. B. Duckett, S. L. Heath, I. G. Khazal, R. N. Perutz, S. Sabo-Etienne and P. L. Timmins, Platinum Bis(tricyclohexylphosphine) Silyl Hydride Complexes, *Organometallics*, 2004, **23**, 5744–5756.

62 J. Takaya and N. Iwasawa, Reaction of bis(o-phosphinophenyl)silane with M(PPh3)4 (M = Ni, Pd, Pt): synthesis and structural analysis of [small eta]2-(Si-H) metal(0) and pentacoordinate silyl metal(ii) hydride complexes of the Ni triad bearing a PSiP-pincer ligand, *Dalton Trans.*, 2011, **40**, 8814–8821.

63 N. Nakata, N. Kato, N. Sekizawa and A. Ishii, Si–H Bond Activation of a Primary Silane with a Pt(0) Complex: Synthesis and Structures of Mononuclear (Hydrido)(dihydrosilyl) Platinum(II) Complexes, *Inorganics*, 2017, **5**, 72.

64 A. Naka, T. Mihara, H. Kobayashi and M. Ishikawa, Platinum-Catalyzed Reactions of 2,3-Bis(diisopropylsilyl) thiophene with Alkynes, *ACS Omega*, 2017, **2**, 8517–8525.

65 H. Keipour, V. Carreras and T. Ollevier, Recent progress in the catalytic carbene insertion reactions into the silicon–hydrogen bond, *Org. Biomol. Chem.*, 2017, **15**, 5441–5456.

66 B. D. Bergstrom, L. A. Nickerson, J. T. Shaw and L. W. Souza, Transition Metal Catalyzed Insertion Reactions with Donor/Donor Carbenes, *Angew. Chem., Int. Ed. Engl.*, 2021, **60**, 6864–6878.

67 Z. Liu, J. Huo, T. Fu, H. Tan, F. Ye, M. L. Hossain and J. Wang, Palladium(0)-catalyzed C(sp3)–Si bond formation via formal carbene insertion into a Si–H bond, *Chem. Commun.*, 2018, **54**, 11419–11422.

68 Z. Xu, W.-S. Huang, J. Zhang and L.-W. Xu, Recent Advances in Transition-Metal-Catalyzed Silylations of Arenes with Hydrosilanes: C–X Bond Cleavage or C–H Bond Activation- Synchronized with Si–H Bond Activation, *Synthesis*, 2015, **47**, 3645–3668.

69 Z. Xu and L.-W. Xu, Silylations of Arenes with Hydrosilanes: From Transition-Metal-Catalyzed C-X Bond Cleavage to Environmentally Benign Transition-Metal-Free C-H Bond Activation, *ChemSusChem*, 2015, **8**, 2176–2179.

70 F. Alonso, I. P. Beletskaya and M. Yus, Metal-Mediated Reductive Hydrodehalogenation of Organic Halides, *Chem. Rev.*, 2002, **102**, 4009–4092.

71 S. Bähr, W. Xue and M. Oestreich, C(sp3)–Si Cross-Coupling, *ACS Catal.*, 2019, **9**, 16–24.

72 G. M. Noonan, B. R. Hayter, A. D. Campbell, T. W. Gorman, B. E. Partridge and G. M. Lamont, Expanding the scope of silane-mediated hydrodehalogenation reactions, *Tetrahedron Lett.*, 2013, **54**, 4518–4521.

73 A. Iwata, Y. Toyoshima, T. Hayashida, T. Ochi, A. Kunai and J. Ohshita, PdCl2 and NiCl2-catalyzed hydrogen–halogen exchange for the convenient preparation of bromo- and iodosilanes and germanes, *J. Organomet. Chem.*, 2003, **667**, 90–95.

74 R. Boukherroub, C. Chatgilialoglu and G. Manuel, PdCl2-Catalyzed Reduction of Organic Halides by Triethylsilane, *Organometallics*, 1996, **15**, 1508–1510.

75 A. Kunai, T. Sakurai, E. Toyoda, M. Ishikawa and Y. Yamamoto, Versatile Method for the Synthesis of Iodosilanes, *Organometallics*, 1994, **13**, 3233–3236.

76 X.-F. Bai, T. Song, W.-H. Deng, Y.-L. Wei, L. Li, C.-G. Xia and L.-W. Xu, (EtO)3SiH-Promoted Palladium-Catalyzed Isomerization of Olefins: Convenient Synthesis of Internal Alkenes from Terminal Alkenes, *Synlett*, 2014, **25**, 417–422.

77 M. Mirza-Aghayan, R. Boukherroub, M. Bolourtchian, M. Hoseini and K. Tabar-Hydar, A novel and efficient method for double bond isomerization, *J. Organomet. Chem.*, 2003, **678**, 1–4.

78 M. Mirza-Aghayan, R. Boukherroub and M. Bolourtchian, A mild and efficient palladium–triethylsilane system for reduction of olefins and carbon–carbon double bond isomerization, *Appl. Organomet. Chem.*, 2006, **20**, 214–219.

79 X.-F. Bai, L.-W. Xu, L.-S. Zheng, J.-X. Jiang, G.-Q. Lai and J.-Y. Shang, Aromatic-Amide-Derived Olefins as a Springboard: Isomerization-Initiated Palladium-Catalyzed Hydrogenation of Olefins and Reductive Decarbonylation of Acyl Chlorides with Hydrosilane, *Chem.–Eur. J.*, 2012, **18**, 8174–8179.

80 M. Mirza-Aghayan, R. Boukherroub and M. Rahimifard, Efficient method for the reduction of carbonyl compounds by triethylsilane catalyzed by PdCl2, *J. Organomet. Chem.*, 2008, **693**, 3567–3570.

81 T. Matsumura, T. Niwa and M. Nakada, Pd-catalyzed reductive cleavage of alkyl aryl sulfides with triethylsilane that is accelerated by trialkylsilyl chloride, *Tetrahedron Lett.*, 2012, **53**, 4313–4316.

82 R. C. Boyle, J. T. Mague and M. J. Fink, The First Stable Mononuclear Silyl Palladium Hydrides, *J. Am. Chem. Soc.*, 2003, **125**, 3228–3229.

83 R. C. Boyle, D. Pool, H. Jacobsen and M. J. Fink, Dynamic Processes in Silyl Palladium Complexes: Evidence for Intermediate Si−H and Si−Si σ-Complexes, *J. Am. Chem. Soc.*, 2006, **128**, 9054–9055.

84 N. Nakata, S. Fukazawa, N. Kato and A. Ishii, Palladium(II) Hydrido Complexes Having a Primary Silyl or Germyl Ligand: Synthesis, Crystal Structures, and Dynamic Behavior, *Organometallics*, 2011, **30**, 4490–4493.

85 B. J. Barrett and V. M. Iluc, An Adaptable Chelating Diphosphine Ligand for the Stabilization of Palladium and Platinum Carbenes, *Organometallics*, 2017, **36**, 730–741.

86 B. J. Barrett and V. M. Iluc, Metal-ligand cooperation between palladium and a diphosphine ligand with an olefinic backbone, *Inorg. Chim. Acta*, 2017, **460**, 35–42.

87 H. Jacobsen and M. J. Fink, Tuning the Palladium−Silicon Bond: Bond Analysis of Bisphosphine Silyl Palladium Hydrides, *Organometallics*, 2006, **25**, 1945–1952.

88 S. Sakaki, M. Ogawa and M. Kinoshita, A Theoretical Study on the Oxidative Addition of an Si-X Bond (X = H or Si) to

M(PH3)2 (M = Pd or Pt). A Comparison of the Reactivity between Pt(PH3)2 and Pd(PH3)2, *J. Phys. Chem.*, 1995, **99**, 9933–9939.

89 V. M. Iluc and G. L. Hillhouse, Snapshots of the oxidative-addition process of silanes to nickel(0), *Tetrahedron*, 2006, **62**, 7577–7582.

90 E. E. Smith, G. Du, P. E. Fanwick and M. M. Abu-Omar, Dehydrocoupling of Organosilanes with a Dinuclear Nickel Hydride Catalyst and Isolation of a Nickel Silyl Complex, *Organometallics*, 2010, **29**, 6527–6533.

91 T. Zell, T. Schaub, K. Radacki and U. Radius, Si-H Activation of hydrosilanes leading to hydrido silyl and bis(silyl) nickel complexes, *Dalton Trans.*, 2011, **40**, 1852–1854.

92 D. Schmidt, T. Zell, T. Schaub and U. Radius, Si-H bond activation at {(NHC)2Ni0} leading to hydrido silyl and bis(silyl) complexes: a versatile tool for catalytic Si-H/D exchange, acceptorless dehydrogenative coupling of hydrosilanes, and hydrogenation of disilanes to hydrosilanes, *Dalton Trans.*, 2014, **43**, 10816–10827.

93 W. D. Jones, Isotope Effects in C−H Bond Activation Reactions by Transition Metals, *Acc. Chem. Res.*, 2003, **36**, 140–146.

94 G. Parkin, Temperature-Dependent Transitions Between Normal and Inverse Isotope Effects Pertaining to the Interaction of H−H and C−H Bonds with Transition Metal Centers, *Acc. Chem. Res.*, 2009, **42**, 315–325.

95 U. Schubert, in *Adv. Organomet. Chem.*, ed. F. G. A. Stone and R. West, Academic Press, 1990, vol. 30, pp. 151–187.

96 G. I. Nikonov, in *Adv. Organomet. Chem.*, ed. R. West, A. F. Hill and F. G. A. Stone, Academic Press, 2005, vol. 53, pp. 217–309.

97 R. Beck and S. A. Johnson, Structural Similarities in Dinuclear, Tetranuclear, and Pentanuclear Nickel Silyl and Silylene Complexes Obtained via Si–H and Si–C Activation, *Organometallics*, 2012, **31**, 3599–3609.

98 S. B. Duckett and R. N. Perutz, Thermal and photochemical reactions of rhodium(trialkylsilyl)hydride complexes: NMR and bonding of poly(silyl)(hydride) complexes, *J. Chem. Soc., Chem. Commun.*, 1991, 28–31.

99 S. B. Duckett and R. N. Perutz, Mechanism of homogeneous hydrosilation of alkenes by (.eta.5-cyclopentadienyl) rhodium, *Organometallics*, 1992, **11**, 90–98.

100 S. Wu, X. Li, Z. Xiong, W. Xu, Y. Lu and H. Sun, Synthesis and Reactivity of Silyl Iron, Cobalt, and Nickel Complexes Bearing a [PSiP]-Pincer Ligand via Si–H Bond Activation, *Organometallics*, 2013, **32**, 3227–3237.

101 J. Takaya and N. Iwasawa, Bis(o-phosphinophenyl)silane as a Scaffold for Dynamic Behavior of H−Si and C−Si Bonds with Palladium(0), *Organometallics*, 2009, **28**, 6636–6638.

102 S. J. Mitton and L. Turculet, Mild Reduction of Carbon Dioxide to Methane with Tertiary Silanes Catalyzed by Platinum and Palladium Silyl Pincer Complexes, *Chem.–Eur. J.*, 2012, **18**, 15258–15262.

103 S. J. Mitton, R. McDonald and L. Turculet, Synthesis and Characterization of Neutral and Cationic Platinum(II) Complexes Featuring Pincer-like Bis(phosphino)silyl Ligands: Si−H and Si−Cl Bond Activation Chemistry, *Organometallics*, 2009, **28**, 5122–5136.

104 J. Mullay, Atomic and group electronegativities, *J. Am. Chem. Soc.*, 1984, **106**, 5842–5847.

105 L. Yang, D. R. Powell and R. P. Houser, Structural variation in copper(i) complexes with pyridylmethylamide ligands: structural analysis with a new four-coordinate geometry index, τ4, *Dalton Trans.*, 2007, 955–964.

106 A. Okuniewski, D. Rosiak, J. Chojnacki and B. Becker, Coordination polymers and molecular structures among complexes of mercury(II) halides with selected 1-benzoylthioureas, *Polyhedron*, 2015, **90**, 47–57.

107 F. R. Hartley, The cis- and trans-effects of ligands, *Chem. Soc. Rev.*, 1973, **2**, 163–179.

108 J. Chatt, C. Eaborn and S. Ibekwe, Silicon, a ligand atom of exceptionally high trans-effect, *Chem. Commun.*, 1966, 700–701.

109 T. G. Appleton, H. C. Clark and L. E. Manzer, The trans-influence: its measurement and significance, *Coord. Chem. Rev.*, 1973, **10**, 335–422.

110 M. Wolfsberg, Theoretical evaluation of experimentally observed isotope effects, *Acc. Chem. Res.*, 1972, **5**, 225–233.

111 D. G. Churchill, K. E. Janak, J. S. Wittenberg and G. Parkin, Normal and Inverse Primary Kinetic Deuterium Isotope Effects for C−H Bond Reductive Elimination and Oxidative Addition Reactions of Molybdenocene and Tungstenocene Complexes: Evidence for Benzene σ-Complex Intermediates, *J. Am. Chem. Soc.*, 2003, **125**, 1403–1420.

112 J. W. Raebiger, A. Miedaner, C. J. Curtis, S. M. Miller, O. P. Anderson and D. L. DuBois, Using Ligand Bite Angles To Control the Hydricity of Palladium Diphosphine Complexes, *J. Am. Chem. Soc.*, 2004, **126**, 5502–5514.

113 E. Buncel and T. K. Venkatachalam, Carbanion mechanisms XXI. Solution acidity of triphenylsilane, *J. Organomet. Chem.*, 2000, **604**, 208–210.

114 S. M. Reid and M. J. Fink, Reductive Routes to Dinuclear d10−d10 Palladium(0) Complexes and Their Redistribution Equilibria in Solution, *Organometallics*, 2001, **20**, 2959–2961.

115 G. Parkin, Applications of deuterium isotope effects for probing aspects of reactions involving oxidative addition and reductive elimination of H–H and C–H bonds, *J. Labelled Compd. Radiopharm.*, 2007, **50**, 1088–1114.

116 F. Abu-Hasanayn, K. Krogh-Jespersen and A. S. Goldman, Theoretical study of primary and secondary deuterium equilibrium isotope effects for hydrogen and methane addition to iridium complex trans-Ir(PR3)2(CO)X, *J. Am. Chem. Soc.*, 1993, **115**, 8019–8023.

117 M. Gómez-Gallego and M. A. Sierra, Kinetic Isotope Effects in the Study of Organometallic Reaction Mechanisms, *Chem. Rev.*, 2011, **111**, 4857–4963.

118 Y. Tsuji and Y. Obora, Structure and fluxional behavior of platinum and palladium complexes having M-Si or M-Sn (M=Pt or Pd) inter-element linkages, *J. Organomet. Chem.*, 2000, **611**, 343–348.

119 S. F. Vyboishchikov and G. I. Nikonov, Rhodium Silyl Hydrides in Oxidation State +5: Classical or Nonclassical?, *Organometallics*, 2007, **26**, 4160–4169.
120 F. P. Gasparro and N. H. Kolodny, NMR determination of the rotational barrier in N,N-dimethylacetamide. A physical chemistry experiment, *J. Chem. Educ.*, 1977, **54**, 258.
121 K. C. Ramey, D. J. Louick, P. W. Whitehurst, W. B. Wise, R. Mukherjee and R. M. Moriarty, A line width method for determining chemical exchange rates from NMR spectra, *Org. Magn. Reson.*, 1971, **3**, 201–216.
122 H. Yamashita and Y. Uchimaru, Highly efficient palladium catalyst system for addition of trihydrosilanes to acetylenes and its application to thermally stable polycarbosilane synthesis, *Chem. Commun.*, 1999, 1763–1764.
123 D. Motoda, H. Shinokubo and K. Oshima, Efficient Pd(0)-catalyzed hydrosilylation of alkynes with triorganosilanes, *Synlett*, 2002, 1529–1531.
124 H. Azizian, K. R. Dixon, C. Eaborn, A. Pidcock, N. M. Shuaib and J. Vinaixa, Dynamic stereochemistry of cis-[PtH(SiR3)(PPh3)2]. Spontaneous ligand interchange with retentilon of nuclear spin–spin correlation, *J. Chem. Soc., Chem. Commun.*, 1982, 1020–1022.
125 J. D. Feldman, G. P. Mitchell, J.-O. Nolte and T. D. Tilley, Synthesis and study of platinum silylene complexes of the type (R3P)2Pt=SiMes2 (Mes = 2,4,6-trimethylphenyl), *Can. J. Chem.*, 2003, **81**, 1127–1136.